



# Evidence for a deep mantle source for EM and HIMU domains from integrated geochemical and geophysical constraints



M.G. Jackson<sup>a,\*</sup>, T.W. Becker<sup>b</sup>, J.G. Konter<sup>c</sup>

<sup>a</sup> Department of Earth Science, University of California Santa Barbara, Santa Barbara, CA, 93106-9630, USA

<sup>b</sup> Institute for Geophysics and Department of Geological Sciences, Jackson School of Geosciences, The University of Texas at Austin, University Station, C1160, Austin, TX 78712-0254, USA

<sup>c</sup> Dept. of Geology and Geophysics, School of Ocean and Earth Science and Technology, University of Hawaii, Manoa, 1680 East-West Rd, Honolulu, HI 96822, USA

## ARTICLE INFO

### Article history:

Received 2 September 2017

Received in revised form 22 November 2017

Accepted 28 November 2017

Available online xxxx

Editor: T.A. Mather

### Keywords:

mantle plumes  
mantle geochemistry  
seismic tomography  
volcanic hotspot  
mantle end members  
ocean island basalts

## ABSTRACT

Subduction of oceanic and continental crust (and associated sediments) into the mantle over geologic time generates mantle domains with geochemically distinct signatures, referred to as HIMU (high “ $\mu$ ”, where  $\mu = {}^{238}\text{U}/{}^{204}\text{Pb}$ ) and EM (enriched mantle) domains. Identification of EM and HIMU geochemical signatures in hotspot lavas provides evidence that subducted crustal materials are recycled into the source of hotspots. It remains uncertain where these materials are located in the mantle, and a key question is whether upwelling mantle plumes are required to transport mantle domains with EM and HIMU signatures to the shallow mantle beneath hotspots. Therefore, this study evaluates relationships between extreme EM and HIMU compositions at oceanic hotspots and the presence (or absence) of seismically-constrained mantle plumes beneath the hotspots. We draw on three existing plume catalogs based on global seismic shear-wave velocity models, and these plume catalogs indicate the presence or absence of a plume beneath each of 42 oceanic hotspots. From each hotspot, we select a lava with the highest  ${}^{206}\text{Pb}/{}^{204}\text{Pb}$  composition and one with the lowest  ${}^{143}\text{Nd}/{}^{144}\text{Nd}$  composition.

We show that hotspots associated with seismically defined plumes show a greater likelihood of hosting lavas with either extreme EM ( ${}^{143}\text{Nd}/{}^{144}\text{Nd} \leq 0.512630$ ) or extreme HIMU ( ${}^{206}\text{Pb}/{}^{204}\text{Pb} \geq 20.0$ ) compositions than hotspots not associated with plumes, but HIMU hotspots show a stronger association with plumes than EM hotspots. The significance of the relationship between plumes and extreme geochemical signatures at hotspots improves if extreme EM and HIMU compositions are considered together instead of separately: hotspots sourced by mantle plumes are even more likely to exhibit extreme EM or extreme HIMU signatures than hotspots not sourced by plumes. The significance tests also show that hotspots with extreme EM or HIMU compositions are more likely to be associated with mantle plumes than hotspots that lack extreme geochemical signatures. A relationship between seismically detected deep mantle plumes and the presence of extreme EM or HIMU compositions at hotspots provides evidence for a deep mantle source for these geochemical domains.

© 2017 Elsevier B.V. All rights reserved.

## 1. Introduction

Geochemists have made great strides in characterizing the geochemical diversity of the accessible mantle by geochemical interrogation of lavas generated by mantle melting (Zindler and Hart, 1986; Hart, 1988; Hofmann, 1997; Stracke, 2012; White, 2015). However, the distribution of geochemical reservoirs in the mantle remains poorly constrained. This is because geochemistry does not provide unique constraints on the depth (or geometry) of origin of the geochemical domains sampled by plumes upwelling

beneath volcanic hotspots. While seismic models provide insights into the structure of the Earth's mantle, such models are not able to uniquely resolve chemical heterogeneities in the mantle. Therefore, the geochemical structure of the Earth's mantle remains poorly constrained, and the depth of mantle domains hosting extreme geochemical compositions—including the EM and HIMU reservoirs—remains unknown.

Seismically anomalous regions in the mantle have long been linked with the extreme geochemical signatures in hotspot lavas (e.g., Castillo, 1988). More recently work has established links between the composition of hotspot lavas and seismically observed structures in the Earth's interior (e.g., Hoernle et al., 1995; Konter and Becker, 2012; Harðardóttir et al., 2017). However, dur-

\* Corresponding author.

E-mail address: jackson@geol.ucsb.edu (M.G. Jackson).

ing the three decades since the initial landmark discovery of [Castillo \(1988\)](#), geochemical datasets have expanded significantly, and now include a larger number of hotspots that sample a wider geographic distribution. Additionally, new, higher-resolution seismic and geodynamic models of mantle plumes (e.g., [Boschi et al., 2007](#); [French and Romanowicz, 2015](#)) provide key insights into the structure and dynamics of the Earth's interior. It is timely to re-examine and further explore the links between the geochemistry of hotspot lavas and seismic models of mantle structures in order to better constrain the geochemical structure and thermo-chemical evolution of the mantle (cf. [Konter and Becker, 2012](#)).

This study seeks to address a key question that lies at the intersection of geochemistry, seismology, and geodynamics: are seismically-constrained mantle plumes associated with hotspots that have distinct radiogenic isotopic compositions? Mantle geochemists frequently refer to particular Sr, Nd and Pb radiogenic isotopic compositions in hotspots lavas as “plume signatures”, but whether or not specific heavy radiogenic isotopic signatures are actually associated with seismically observed mantle plumes appears to not have been systematically tested.

The geographic correspondence of geochemically enriched hotspots at the Earth's surface with the predominantly degree-two, low shear-wave velocity provinces in the deep mantle (sometimes referred to as LLSVPs) was interpreted as evidence that these provinces host enriched, subducted components that are conveyed to the shallow mantle beneath hotspots via upwelling mantle plumes ([Castillo, 1988](#)). In this model, extreme mantle domains created by subduction of continental and oceanic crust, including EM ([White and Hofmann, 1982](#)) and HIMU ([Hofmann and White, 1982](#)) reservoirs, respectively, will be concentrated in the deep lower mantle. Therefore, if EM and HIMU domains are concentrated in the deep mantle, then hotspots fed by seismically-observed mantle plumes that emerge from the lower mantle (referred to as plume-related hotspots below) should be more likely to sample EM and HIMU domains than mid-ocean ridges and hotspots that are not sourced by plumes (referred to as non-plume hotspots), which sample only the upper mantle. We evaluate whether extreme EM or HIMU signatures are more likely to be associated with oceanic hotspots that overlie seismically observed plumes, or whether these geochemical signatures are just as likely to be found in hotspots that are not sourced by seismically observed plumes.

## 2. Background

There are several mantle endmembers that have been identified in oceanic lavas based on their radiogenic isotopic compositions ([Zindler and Hart, 1986](#)): EM1 (characterized by intermediate  $^{87}\text{Sr}/^{86}\text{Sr}$ , low  $^{143}\text{Nd}/^{144}\text{Nd}$ ,  $^{206}\text{Pb}/^{204}\text{Pb}$ ), EM2 (enriched mantle II; low  $^{143}\text{Nd}/^{144}\text{Nd}$ , intermediate  $^{206}\text{Pb}/^{204}\text{Pb}$ , high  $^{87}\text{Sr}/^{86}\text{Sr}$ ), HIMU (high  $\mu = ^{238}\text{U}/^{204}\text{Pb}$ ; high  $^{206}\text{Pb}/^{204}\text{Pb}$ , intermediate  $^{143}\text{Nd}/^{144}\text{Nd}$ , low  $^{87}\text{Sr}/^{86}\text{Sr}$ ), DMM (depleted MORB mantle; high  $^{143}\text{Nd}/^{144}\text{Nd}$ , low  $^{87}\text{Sr}/^{86}\text{Sr}$ , low  $^{206}\text{Pb}/^{204}\text{Pb}$ ), and a common component with elevated  $^3\text{He}/^4\text{He}$  that has been referred to as FOZO (Focus Zone; [Hart et al., 1992](#)), PHEM (Primitive Helium Mantle; [Farley et al., 1992](#)) or C ([Hanan and Graham, 1996](#)).

In this work, we build on the results by [Konter and Becker \(2012\)](#), who performed first-order correlation tests for 27 parameters (including geochemical compositions, seismic velocities at depth, etc.) for a global oceanic hotspot dataset. They found that the C (Common; [Hanan and Graham, 1996](#)) and EM1 (enriched mantle I) geochemical components display statistically significant relationships with, 1), shallow seismic velocities, and, 2), the maximum depth to which a plume can be resolved (i.e., plume depth extent; [Boschi et al., 2007](#)). [Konter and Becker's \(2012\)](#) suggestion to use helium isotopes to investigate the relationship be-

tween shallow mantle seismic shear-wave velocity anomalies (i.e., at 200 km depth) and the C component at hotspots was pursued by [Jackson et al. \(2017\)](#).

Here, we take a different approach to that taken by [Konter and Becker \(2012\)](#), who used correlations based on small compositional (EM1, EM2, HIMU or C) subsets of hotspots to identify whether hotspot geochemistry correlates with geophysical parameters. Instead, we simply score whether hotspots associated with seismically-observed plumes have a greater tendency than non-plume (i.e., no seismically-observed plume) hotspots to be associated with extreme EM or HIMU signatures.

## 3. Methods

In this study, we select lavas with the lowest  $^{143}\text{Nd}/^{144}\text{Nd}$ , and lavas with highest  $^{206}\text{Pb}/^{204}\text{Pb}$ , from each of 42 oceanic hotspots. We use these data to identify the magnitude of EM and HIMU signatures expressed in lavas at each hotspot. Below we outline the hotspots that are considered in this study, and the methods for identifying geochemically extreme EM and HIMU compositions at each hotspot.

### 3.1. Hotspot catalog

This study explores the geochemical endmember compositions in lavas erupted at major hotspots globally. The study draws on the hotspot database from [King and Adam \(2014\)](#). To this database we add the Manus Basin plume: a plume conduit identified as being related to the Manus Basin ([Jackson et al., 2017](#)) was reported by [French and Romanowicz \(2015\)](#) (who referred to this as the “Indonesia” conduit), and the plume is located near a location where high  $^3\text{He}/^4\text{He}$  lavas were discovered ([Macpherson et al., 1998](#)). Sr, Nd, and Pb isotopic compositions of hotspot lavas associated with continents are not considered here owing to the possibility of continental overprinting of the radiogenic isotopic signatures of hotspot mantle signals as a result of magmatic processes operating within the crust. Therefore, eight of the continental hotspots in the [King and Adam \(2014\)](#) catalog are not shown in [Tables 1 and 2](#) (and Supplementary Tables 1 and 2): Australia East, Darfur, Eifel, Hoggar, Raton-Jemez, Tibesti, Yellowstone, and Afar (we have identified Afar volcanism with the hotspot location further to the southeast, often identified as East Africa). Only lavas with Sr, Nd and Pb isotopes measured on the same sample are used in this study, as this provides a more complete geochemical context. Thus, four oceanic hotspots in the [King and Adam \(2014\)](#) database that do not yet have a complete set of published heavy radiogenic isotopic data—Vema, Bermuda, Tasmanid-Tasman Central, and Lord Howe-Tasman East—are not examined here. The remaining 42 oceanic hotspots have available Sr, Nd and Pb isotopic data, and the data are presented in [Tables 1 and 2](#). The global distribution, and the extreme low  $^{143}\text{Nd}/^{144}\text{Nd}$  and high  $^{206}\text{Pb}/^{204}\text{Pb}$  isotopic compositions, of these 42 hotspots are shown in [Fig. 1](#).

### 3.2. Selection of lavas with the most extreme EM and HIMU signatures

Of the 42 oceanic hotspots explored here, many exhibit a range in geochemical signatures. In these cases no single lava captures the geochemical diversity of compositions at a given hotspot (e.g., Macdonald, Samoa, Hawaii, etc.). In order to better represent the geochemical extremes at each hotspot, we selected a lava with the highest  $^{206}\text{Pb}/^{204}\text{Pb}$  and a lava with the lowest  $^{143}\text{Nd}/^{144}\text{Nd}$  from each hotspot. However, in cases where a single lava exhibits both the highest  $^{206}\text{Pb}/^{204}\text{Pb}$  and the lowest  $^{143}\text{Nd}/^{144}\text{Nd}$  from a hotspot (e.g., Cobb-Axial-Juan de Fuca, Juan Fernandez, etc.), it was not necessary to select two lavas. In Supplementary [Fig. 1](#), 42 separate plots of  $^{143}\text{Nd}/^{144}\text{Nd}$  versus  $^{206}\text{Pb}/^{204}\text{Pb}$  show the full range

**Table 1**  
Sr, Nd and Pb isotopic compositions for the lowest (most geochemically enriched)  $^{143}\text{Nd}/^{144}\text{Nd}$  lavas from each of 42 oceanic hotspots.

Hotspot <sup>a</sup>	Hotspot latitude <sup>a</sup>	Hotspot latitude <sup>a</sup>	Plume/no plume? FR catalogue <sup>b</sup>	Plume/no plume? B-1 catalogue <sup>b</sup>	Plume/No Plume? B-2 catalogue <sup>b</sup>	$^{87}\text{Sr}/^{86}\text{Sr}^{\text{d}}$	$^{143}\text{Nd}/^{144}\text{Nd}$	$^{206}\text{Pb}/^{204}\text{Pb}$	$^{207}\text{Pb}/^{204}\text{Pb}$	$^{208}\text{Pb}/^{204}\text{Pb}$
Arago	−23.5	−150.7	no plume	–	–	0.704661	0.512766	19.58	15.64	39.58
Amsterdam-St. Paul	−37	78	no plume	–	–	0.705360	0.512590	17.76	15.54	38.47
Ascension	−8	−14	plume	–	–	0.702913	0.513003	19.66	15.66	39.31
Azores	38	−28	plume	plume	plume	0.705475	0.512667	20.04	15.80	40.58
Baja-Guadalupe	27	−113	no plume	no plume	no plume	0.704150	0.512887	18.52	15.60	38.27
Balleny	−67.4	164.7	no plume	plume	plume	0.703000	0.512960	19.76	15.59	39.40
Bouvet	−54.4	3.4	plume	–	–	0.703680	0.512842	19.53	15.65	39.16
Bowie-Pratt Welker	49.5	−130	no plume	no plume	no plume	0.702450	0.513041	18.98	15.59	38.49
Cameroon	−1	6	plume	plume	plume	0.703390	0.512723	19.98	15.62	39.84
Canary	28	−17	plume	plume	plume	0.703210	0.512740	19.05	15.53	38.81
Cape Verde	15	−24	plume	plume	plume	0.703934	0.512606	18.74	15.53	38.66
Caroline	5.3	163	plume	plume	plume	0.703472	0.512924	18.44	15.51	38.33
Cobb-Axial-Juan de Fuca	43.6	−128.7	no plume	no plume	no plume	0.702839	0.513014	19.54	15.58	38.92
Comores	−12	44	plume	plume	plume	0.703910	0.512630	19.35	15.55	39.41
Crozet	−46	50	plume	–	–	0.704170	0.512822	18.96	15.59	39.15
Discovery	−44.5	−6.5	no plume	–	–	0.706682	0.512207	17.95	15.63	38.66
Easter	−27	−109	plume	plume	plume	0.703339	0.512783	20.44	15.72	40.47
Fernando de Noronha	−4	−32	no plume	no plume	no plume	0.704910	0.512712	19.14	15.57	39.05
Galapagos	−0.4	−92	plume	no plume	plume	0.703420	0.512877	19.43	15.57	38.99
Great Meteor-New England <sup>c</sup>	31	−28.5	no plume	plume	plume	0.703230	0.512672	19.89	15.60	39.74
Hawaii	18.9	−155.3	plume	plume	plume	0.704510	0.512540	17.75	15.39	37.79
Heard	−49	63	plume	plume	plume	0.706115	0.512483	17.93	15.56	38.47
Iceland	64.6	−17.6	plume	plume	plume	0.703429	0.512893	19.24	15.54	38.84
Jan Mayen	71.7	−8	no plume	plume	plume	0.703518	0.512848	18.64	15.46	38.34
Juan Fernandez	−34	−79	plume	no plume	no plume	0.703779	0.512818	19.21	15.63	39.10
Louisville	−53.5	−141.2	plume	no plume	no plume	0.704210	0.512834	19.25	15.61	39.12
Macdonald	−29	−140.4	plume	plume	plume	0.704338	0.512687	18.95	15.62	39.00
Madeira	32.7	−17.5	no plume	–	–	0.702900	0.512820	19.51	15.57	39.20
Manus Basin-“Indonesia”	−3.8	149.7	plume	–	–	0.703350	0.512959	18.52	15.50	38.33
Marion-Prince Edward	−46.75	37.75	no plume	plume	no plume	0.703390	0.512880	18.56	15.55	38.40
Marquesas	−11.5	−137.5	plume	plume	plume	0.705506	0.512690	19.13	15.63	39.18
Martin Vas-Trindade	−20	−29	no plume	no plume	no plume	0.704130	0.512720	19.01	15.59	39.08
Meteor-Shona <sup>c</sup>	−52	1	no plume	plume	no plume	0.705590	0.512400	18.37	15.63	38.76
Pitcairn	−25.3	−129.3	plume	plume	plume	0.705105	0.512333	17.64	15.49	39.02
Rarotonga	−21.5	−159.7	no plume	–	–	0.704366	0.512629	18.26	15.52	38.72
Reunion	−21	55.5	plume	plume	plume	0.704115	0.512771	18.97	15.59	39.03
Samoa	−14.3	−169	plume	plume	plume	0.720469	0.512287	18.95	15.65	39.42
San Felix	−26	−80	plume	plume	no plume	0.704122	0.512552	19.31	15.60	39.33
Societies	−18.3	−148	plume	plume	plume	0.706310	0.512565	19.25	15.59	38.80
Socorro-Revillagigedo	19	−111	no plume	no plume	no plume	0.703126	0.512889	19.10	15.59	38.75
St. Helena	−17	−10	plume	no plume	no plume	0.702910	0.512870	20.96	15.81	40.18
Tristan-Gough <sup>c</sup>	−40.3	−10	plume	plume	plume	0.705559	0.512203	17.35	15.45	38.01

<sup>a</sup> The hotspots and locations are from King and Adam (2014). Manus Basin is added to the plume catalogue here, after Jackson et al. (2017).

<sup>b</sup> Whether or not a hotspot is associated with a plume is based on three different plume catalogues from French and Romanowicz (2015) and Boschi et al. (2007). These plume catalogues are discussed in detail in Jackson et al. (2017). If a hotspot is associated with a plume in one of the catalogues, this is recorded as “plume” in the table. If no plume was detected, this is recorded as “no plume” in the table. If the presence of a plume was not evaluated, this is recorded as “–” in the table.

<sup>c</sup> Used age corrected data.

<sup>d</sup> Sample identification and references for lavas shown here are provided in Supplementary Table 1.

**Table 2**  
Sr, Nd and Pb isotopic compositions for lavas with the highest  $^{206}\text{Pb}/^{204}\text{Pb}$  from each of 42 oceanic hotspots.

Hotspot <sup>a</sup>	Hotspot latitude <sup>a</sup>	Hotspot latitude <sup>a</sup>	Plume/no plume? FR catalogue <sup>b</sup>	Plume/no plume? B-1 catalogue <sup>b</sup>	Plume/No Plume? B-2 catalogue <sup>b</sup>	$^{87}\text{Sr}/^{86}\text{Sr}^{\text{d}}$	$^{143}\text{Nd}/^{144}\text{Nd}$	$^{206}\text{Pb}/^{204}\text{Pb}$	$^{207}\text{Pb}/^{204}\text{Pb}$	$^{208}\text{Pb}/^{204}\text{Pb}$
Arago	−23.5	−150.7	no plume	–	–	0.703371	0.512918	20.46	15.71	39.98
Amsterdam-St. Paul	−37.0	78.0	no plume	–	–	0.703676	0.512843	19.41	15.65	39.66
Ascension	−8.0	−14.0	plume	–	–	0.702913	0.513003	19.66	15.66	39.31
Azores	38.0	−28.0	plume	plume	plume	0.703752	0.512959	20.51	15.67	39.56
Baja-Guadalupe	27.0	−113.0	no plume	no plume	no plume	0.703260	0.512942	20.30	15.64	40.26
Balleny	−67.4	164.7	no plume	plume	plume	0.703000	0.512960	19.76	15.59	39.40
Bouvet	−54.4	3.4	plume	–	–	0.703680	0.512842	19.53	15.65	39.16
Bowie-Pratt Welker	49.5	−130.0	no plume	no plume	no plume	0.702460	0.513137	19.49	15.57	38.68
Cameroon	−1.0	6.0	plume	plume	plume	0.703330	0.512835	20.52	15.66	40.34
Canary	28.0	−17.0	plume	plume	plume	0.703088	0.512919	20.27	15.65	39.80
Cape Verde	15.0	−24.0	plume	plume	plume	0.703281	0.512906	20.25	15.64	39.36
Caroline	5.3	163.0	plume	plume	plume	0.703475	0.512938	18.84	15.55	38.70
Cobb-Axial-Juan de Fuca	43.6	−128.7	no plume	no plume	no plume	0.702839	0.513014	19.54	15.58	38.92
Comores	−12.0	44.0	plume	plume	plume	0.703190	0.512880	20.42	15.68	40.07
Crozet	−46.0	50.0	plume	–	–	0.703211	0.512952	19.65	15.63	39.28
Discovery	−44.5	−6.5	no plume	–	–	0.705724	0.512445	18.29	15.63	38.77
Easter	−27.0	−109.0	plume	plume	plume	0.703339	0.512783	20.44	15.72	40.47
Fernando de Noronha	−4.0	−32.0	no plume	no plume	no plume	0.703890	0.512840	19.57	15.64	39.36
Galapagos	−0.4	−92.0	plume	no plume	plume	0.703485	0.512951	20.06	15.66	39.78
Great Meteor-New England <sup>c</sup>	31.0	−28.5	no plume	plume	plume	0.703440	0.512695	20.44	15.66	39.83
Hawaii	18.9	−155.3	plume	plume	plume	0.703560	0.513000	18.86	15.61	38.54
Heard	−49.0	63.0	plume	plume	plume	0.704728	0.512729	18.83	15.60	39.27
Iceland	64.6	−17.6	plume	plume	plume	0.703410	0.512994	19.31	15.58	38.99
Jan Mayen	71.7	−8.0	no plume	plume	plume	0.703453	0.512903	18.84	15.51	38.62
Juan Fernandez	−34.0	−79.0	plume	no plume	no plume	0.703779	0.512818	19.21	15.63	39.10
Louisville	−53.5	−141.2	plume	no plume	no plume	0.703280	0.512869	19.61	15.62	39.29
Macdonald	−29.0	−140.4	plume	plume	plume	0.702805	0.512856	21.65	15.83	40.54
Madeira	32.7	−17.5	no plume	–	–	0.702872	0.513016	19.79	15.58	39.47
Manus Basin-“Indonesia”	−3.8	149.7	plume	–	–	0.703204	0.513084	18.78	15.53	38.37
Marion-Prince Edward	−46.8	37.8	no plume	plume	no plume	0.703378	0.512944	18.75	15.56	38.60
Marquesas	−11.5	−137.5	plume	plume	plume	0.702871	0.512916	20.14	15.55	39.72
Martin Vas-Trindade	−20.0	−29.0	no plume	no plume	no plume	0.703740	0.512840	19.50	15.62	39.51
Meteor-Shona	−52.0	1.0	no plume	plume	no plume	0.702740	0.512987	18.92	15.60	38.82
Pitcairn	−25.3	−129.3	plume	plume	plume	0.703492	0.512921	19.55	15.55	39.16
Rarotonga	−21.5	−159.7	no plume	–	–	0.704290	0.512750	18.98	15.56	38.80
Reunion	−21.0	55.5	plume	plume	plume	0.703690	0.512874	19.17	15.60	39.35
Samoa	−14.3	−169.0	plume	plume	plume	0.704426	0.512824	19.47	15.60	39.58
San Felix	−26.0	−80.0	plume	plume	no plume	0.704122	0.512552	19.31	15.60	39.33
Societies	−18.3	−148.0	plume	plume	plume	0.705687	0.512647	19.55	15.68	39.17
Socorro-Revillagigedo	19.0	−111.0	no plume	no plume	no plume	0.703159	0.512901	19.14	15.64	38.86
St Helena	−17.0	−10.0	plume	no plume	no plume	0.702910	0.512870	20.96	15.81	40.18
Tristan-Gough	−40.3	−10.0	plume	plume	plume	0.702810	0.512810	19.86	15.74	39.67

<sup>a</sup> The hotspots and locations are from King and Adam (2014). Manus Basin is added to the plume catalogue here, after Jackson et al. (2017).

<sup>b</sup> Whether or not a hotspot is associated with a plume is based on three different plume catalogues from French and Romanowicz (2015) and Boschi et al. (2007). These plume catalogues are discussed in detail in Jackson et al. (2017). If a hotspot is associated with a plume in one of the catalogues, this is recorded as “plume” in the table. If no plume was detected, this is recorded as “no plume” in the table. If the presence of a plume was not evaluated, this is recorded as “–” in the table.

<sup>c</sup> Used age corrected data.

<sup>d</sup> Sample identification and references for lavas shown here are provided in Supplementary Table 1.

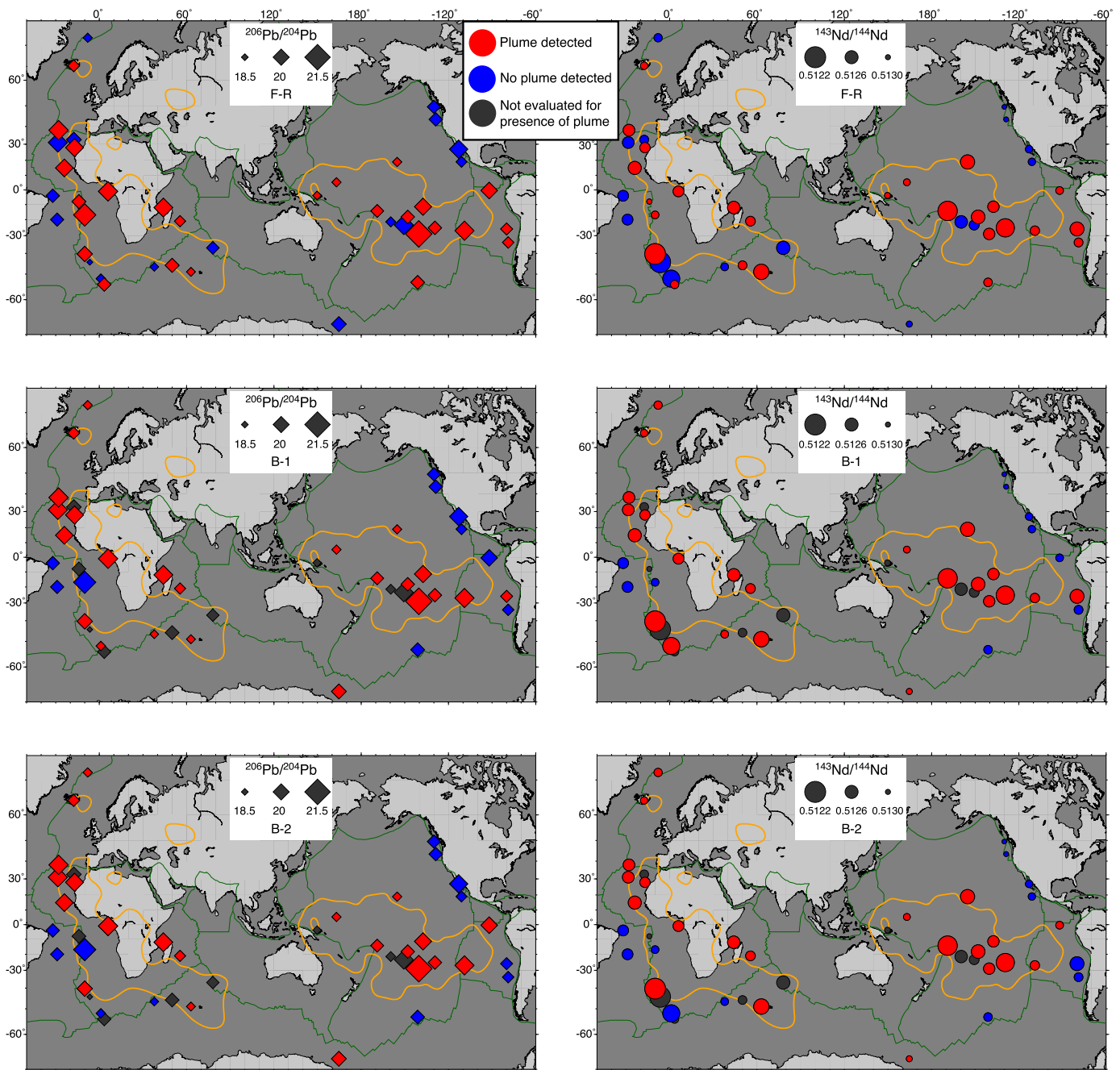


**Fig. 1.** The minimum  $^{143}\text{Nd}/^{144}\text{Nd}$  and maximum  $^{206}\text{Pb}/^{204}\text{Pb}$  isotopic compositions identified at each of the 42 geochemically characterized oceanic hotspots (Tables 1 and 2 and Supplementary Tables 1 and 2) shown on a map. The size of the symbol reflects the magnitude of the geochemical signature: the most geochemically enriched lavas have the lowest  $^{143}\text{Nd}/^{144}\text{Nd}$  and have the largest symbols (smaller symbols represent higher, and therefore more geochemically-depleted,  $^{143}\text{Nd}/^{144}\text{Nd}$ ), and the lavas with the highest  $^{206}\text{Pb}/^{204}\text{Pb}$  have the largest symbols (smaller symbols represent lower  $^{206}\text{Pb}/^{204}\text{Pb}$ ). Three plume catalogs are shown: the FR (French and Romanowicz, 2015) catalog (top panels), the B-1 (Boschi et al., 2007) catalog (middle panels), and the B-2 (Boschi et al., 2007) catalog (bottom panels). Colors of symbols indicate whether the plume catalogs have identified a plume under the hotspot (red symbol), have not identified a plume (blue), or the hotspot was not evaluated for the presence of a plume (black). The  $-1\%$   $\delta V_s$  velocity anomaly at 2850 km, using the SMEAN2 global shear-wave velocity model (modified after Becker and Boschi, 2002, as discussed in Jackson et al., 2017), is shown with an orange line. (For interpretation of the references to color in this figure, the reader is referred to the web version of this article.)

of isotopic variability in lavas from each of the 42 oceanic hotspots, and the extreme lavas with the highest  $^{206}\text{Pb}/^{204}\text{Pb}$  and the lowest  $^{143}\text{Nd}/^{144}\text{Nd}$  from each hotspot are shown for reference.

### 3.2.1. The EM endmember at each hotspot

In Sr, Nd, and Pb radiogenic isotopic space there is a continuum of compositions between the endmember EM1 and EM2 mantle compositions (Stracke et al., 2005), and we do not distinguish between EM1 and EM2 in this study. Instead, this study seeks to find the lava with the lowest (most geochemically enriched)

$^{143}\text{Nd}/^{144}\text{Nd}$  at each hotspot, irrespective of its designation as EM1 or EM2. Note that the  $^{143}\text{Nd}/^{144}\text{Nd}$  ratio is generally preferred as an indicator of the EM source in this study because  $^{87}\text{Sr}/^{86}\text{Sr}$  is not always as reliable of an indicator of EM source compositions: Sr is more fluid-mobile than Nd, and the  $^{87}\text{Sr}/^{86}\text{Sr}$  ratio is more susceptible to modification by assimilation of seawater-derived materials (e.g., Socorro-Revilagigedo hotspot; Bohrsen and Reid, 1997).

We use the chondritic  $^{143}\text{Nd}/^{144}\text{Nd}$  (0.512630; Bouvier et al., 2008) as the threshold value for identifying hotspots with geochemically enriched (EM) compositions, and hotspots with lavas

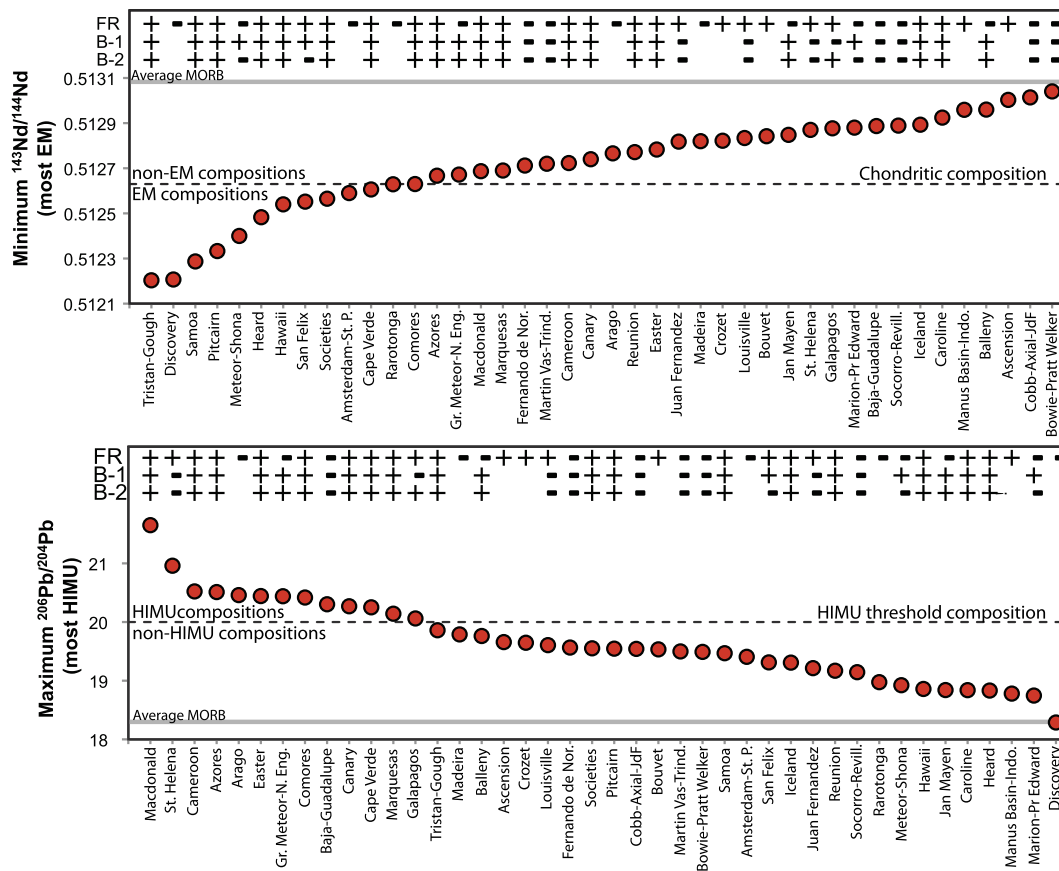


**Fig. 2.** The minimum  $^{143}\text{Nd}/^{144}\text{Nd}$  and maximum  $^{206}\text{Pb}/^{204}\text{Pb}$  compositions identified in lavas at each of the 42 geochemically characterized oceanic hotspots in the database (all hotspot data shown are presented in Tables 1 and 2). The presence of a mantle plume (marked with a “+”) or absence of a mantle plume (marked with a “–”) at a hotspot is shown for three plume catalogs, as discussed in Jackson et al. (2017): FR (French and Romanowicz, 2015) catalog, the B-1 (Boschi et al., 2007) catalog, and the B-2 (Boschi et al., 2007) catalog. If the catalog did not evaluate the presence of a plume beneath a hotspot, no symbol is shown. The average composition of MORB (Gale et al., 2013) is shown with a solid gray line. The cutoff  $^{143}\text{Nd}/^{144}\text{Nd}$  value for EM hotspots (0.512630), and the cutoff  $^{206}\text{Pb}/^{204}\text{Pb}$  value for HIMU hotspots (20.0), are shown with black dashed lines.

that have  $^{143}\text{Nd}/^{144}\text{Nd} \leq 0.512630$  are treated as geochemically enriched in this study. Only 13 of the 42 oceanic hotspots (or ~31%) considered host lavas with geochemically enriched  $^{143}\text{Nd}/^{144}\text{Nd}$  compositions. Most hotspots (29 out of 42) exhibit only geochemically-depleted (i.e.,  $^{143}\text{Nd}/^{144}\text{Nd} > 0.512630$ ) compositions (Fig. 2, Table 1).

### 3.2.2. The HIMU endmember at each hotspot

We also select a lava at each hotspot with the highest  $^{206}\text{Pb}/^{204}\text{Pb}$  ratio. While any strict minimum cutoff  $^{206}\text{Pb}/^{204}\text{Pb}$  value defining the HIMU component is arbitrary, a threshold value of  $^{206}\text{Pb}/^{204}\text{Pb} \geq 20$  is used here to identify hotspots with the most extreme HIMU compositions globally. This threshold appears a conservative choice since it is both higher than DMM and the upper range of  $^{206}\text{Pb}/^{204}\text{Pb}$  values suggested for the FOZO and C components (Hart et al., 1992; Hanan and Graham, 1996). Of the 42 oceanic hotspots with available  $^{206}\text{Pb}/^{204}\text{Pb}$  data, just 13 out of the 42 oceanic hotspots (or ~31%) have maximum  $^{206}\text{Pb}/^{204}\text{Pb} \geq 20$ , and only two hotspots—Macdonald and St. Helena—have  $^{206}\text{Pb}/^{204}\text{Pb} > 20.9$  (Fig. 2, Table 2). Most hotspots (29 out of 42) lack HIMU signatures.

### 3.3. Hotspot classification based on association with seismically-constrained plumes

In Tables 1 and 2, we indicate whether each hotspot is associated with a mantle plume. As discussed in Jackson et al. (2017), we use three different plume catalogs to evaluate the presence or absence of plumes beneath hotspots. First, using a recent, global

seismic shear-wave velocity model, French and Romanowicz (2015) identified 28 low velocity conduits in the mantle beneath known hotspots; we use this plume catalog (the “FR” catalog in the figures and tables) here. Additionally, Boschi et al. (2007) developed a seismic definition for mantle plumes based on the continuity of modeled plume conduits across the mantle in global seismic shear-wave velocity models, and they use a quantity referred to as the “normalized vertical extent” (NVE) of the plume. An NVE value of zero indicates the absence of a continuous vertical plume, while an NVE value of 1 indicates that the plume is continuous across the entire depth of the mantle. We use the Boschi et al. (2007) seismic definition of plumes to generate two plume catalogs using, 1) the SMEAN global seismic shear-wave velocity model (Becker and Boschi, 2002) in the “B-1” (or Boschi-1) catalog and, 2) a suite of global seismic shear-wave velocity models (including SMEAN) in the “B-2” (or Boschi-2) catalog. Conduits with  $\text{NVE} \geq 0.5$  (i.e., spanning at least one-half of the mantle’s depth) are treated as plumes, and conduits with  $\text{NVE} < 0.5$  are not treated as plumes.

The three plume catalogs agree on the presence of a plume at 17 geochemically-characterized oceanic hotspots: Azores, Cameroon, Canary, Cape Verde, Caroline, Comores, Easter, Hawaii, Heard, Iceland, Macdonald, Marquesas, Pitcairn, Reunion, Samoa, Societies, and Tristan-Gough. Similarly, the three plume catalogs agree that there is no plume under the following six geochemically-characterized oceanic hotspots: Baja-Guadalupe, Bowie-Pratt Welker, Cobb-Axial-Juan de Fuca, Fernando de Noronha, Martin Vas-Trindade, and Socorro-Revillagigedo. However, there are hotspots for which the three plume catalogs do not agree

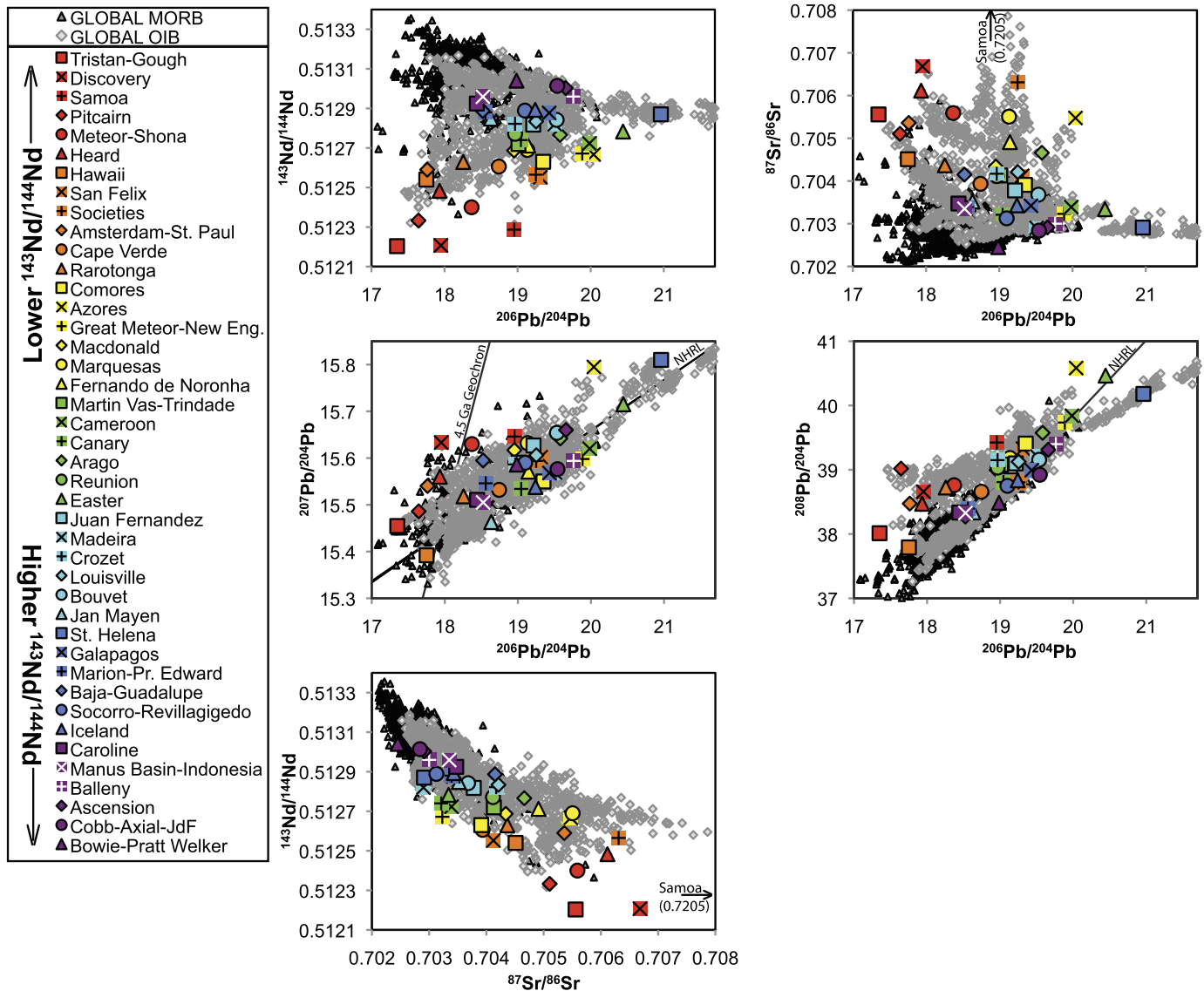


**Fig. 3.** The radiogenic isotopic compositions for lavas with the lowest  $^{143}\text{Nd}/^{144}\text{Nd}$  from each of the 42 geochemically characterized oceanic hotspots are shown in various radiogenic isotopic spaces. These 42 lavas are plotted together with lavas from the global MORB and OIB databases. In the legend, the 42 extreme low  $^{143}\text{Nd}/^{144}\text{Nd}$  samples from each hotspot are organized by increasing  $^{143}\text{Nd}/^{144}\text{Nd}$ , from top to bottom: warmer colors represent lavas with lower  $^{143}\text{Nd}/^{144}\text{Nd}$ , and cooler colors represent lavas with higher  $^{143}\text{Nd}/^{144}\text{Nd}$ . The NHRL (Northern Hemisphere Reference Line) is from Hart (1984). All values are shown in Table 1. (For interpretation of the references to color in this figure, the reader is referred to the web version of this article.)

on the presence or absence of a plume. For example, only one or two of the three seismic models suggest the presence of plumes under the following 10 oceanic hotspots: Balleny, Galapagos, Great Meteor-New England, Jan Mayen, Juan Fernandez, Louisville, Marion-Prince Edward, Meteor-Shona, San Felix, and St. Helena. Finally, Boschi et al. (2007) did not look for the presence of a plume at nine oceanic hotspots: Arago, Discovery, Manus Basin (“Indonesia”), Bouvet, Amsterdam-St. Paul, Crozet, Ascension, Madeira, and Rarotonga. For these hotspots we cannot evaluate whether there is agreement with the French and Romanowicz (2015) model.

#### 4. Observations

##### 4.1. Associations between seismically-constrained mantle plumes and extreme EM and HIMU compositions at hotspots

The Sr, Nd, and Pb radiogenic isotopic compositions of the lowest  $^{143}\text{Nd}/^{144}\text{Nd}$  lava from each of the 42 hotspots are presented

as scatter plots in Fig. 3. The data show that these extreme lavas sample the full spectrum of enriched mantle compositions among global oceanic lavas. Similarly, the radiogenic isotopic compositions of the lava with the highest  $^{206}\text{Pb}/^{204}\text{Pb}$  from each of the 42 hotspots are shown in Fig. 4. Below we evaluate whether extreme EM and HIMU compositions in global hotspot lavas relate to the presence of seismically-constrained mantle plumes sourcing the hotspots.

##### 4.1.1. $^{143}\text{Nd}/^{144}\text{Nd}$ in mantle-derived hotspot lavas: the distribution of enriched mantle (EM) components among plume-related (and non-plume related) hotspots

The minimum  $^{143}\text{Nd}/^{144}\text{Nd}$  ratios of most of the 42 geochemically-characterized hotspots considered here are lower than the value for normal MORB ( $0.513083 \pm 0.000020$ , 95% confidence; this excludes back-arc basin basalts and MORB < 500 km from hotspots) (Gale et al., 2013). Thus, while true geochemical enrichment ( $^{143}\text{Nd}/^{144}\text{Nd} \leq 0.512630$ ) is relatively uncommon at hotspots (i.e., only 13 of the 42 hotspots have lavas with

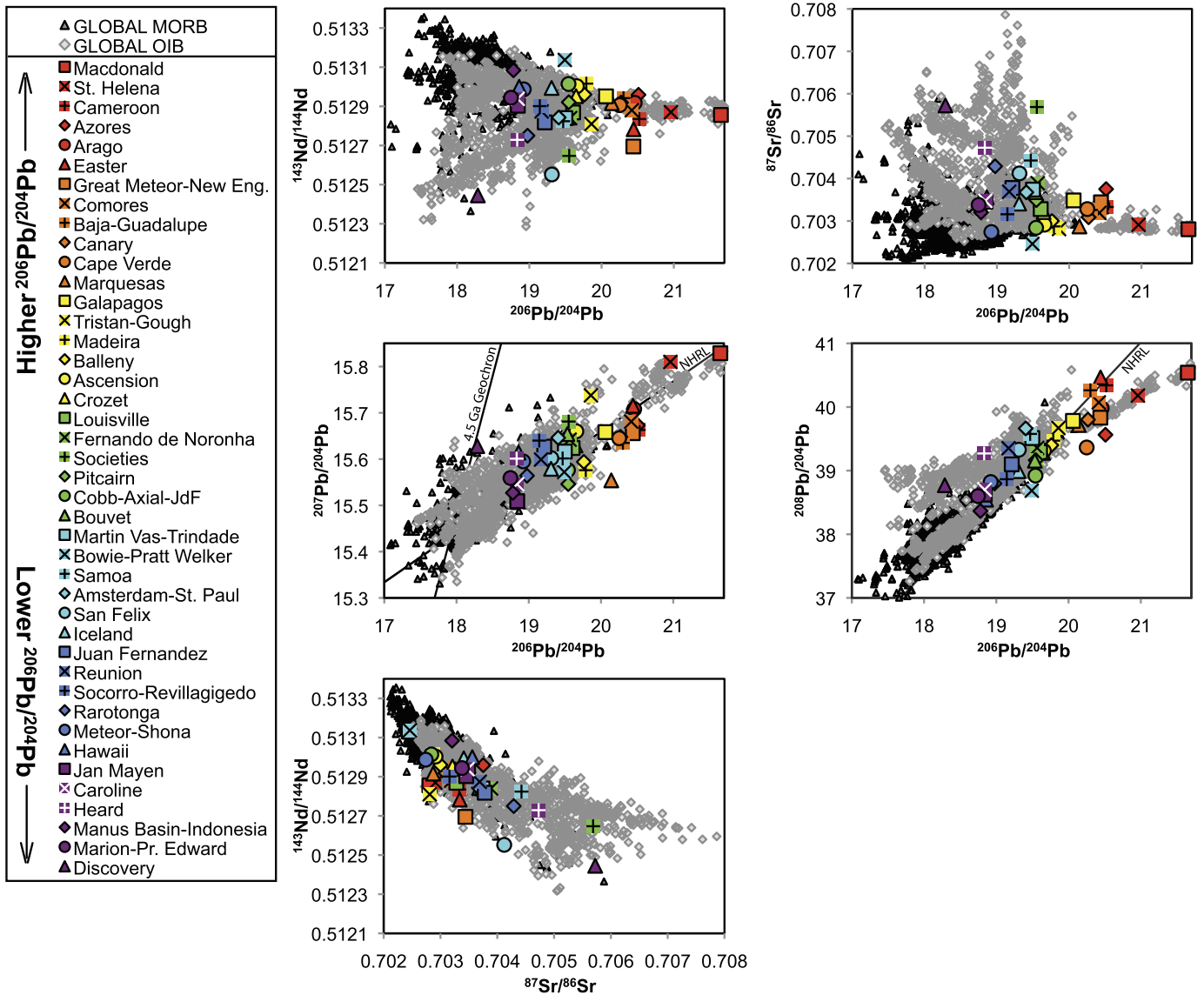


**Fig. 4.** The radiogenic isotopic compositions for the lavas with the highest  $^{206}\text{Pb}/^{204}\text{Pb}$  from each of the 42 geochemically characterized oceanic hotspots are shown in various radiogenic isotopic spaces. These 42 lavas are plotted together with lavas from the global MORB and OIB databases. In the legend, the 42 extreme high  $^{206}\text{Pb}/^{204}\text{Pb}$  samples are organized by decreasing  $^{206}\text{Pb}/^{204}\text{Pb}$ , from top to bottom: warmer colors represent lavas with higher  $^{206}\text{Pb}/^{204}\text{Pb}$ , and cooler colors represent lavas with lower  $^{206}\text{Pb}/^{204}\text{Pb}$ . The NHRL (Northern Hemisphere Reference Line) is from Hart (1984). All values are shown in Table 2. (For interpretation of the references to color in this figure, the reader is referred to the web version of this article.)

$^{143}\text{Nd}/^{144}\text{Nd} \leq 0.512630$ ), oceanic hotspots considered here tend to erupt lavas that sample mantle domains more enriched than the average MORB composition.

To make first-order observations about relationships between the presence (or absence) of mantle plumes and hotspot geochemistry, we first focus on the geochemical characteristics of hotspots where all three plume catalogs agree on the presence (or absence) of a plume beneath the hotspot, as detection of plumes across multiple catalogs may provide more confidence regarding the detection of a plume. Of the 13 hotspots that have geochemically enriched  $^{143}\text{Nd}/^{144}\text{Nd}$  ratios, eight are associated with mantle plumes in all three plume catalogs: Tristan-Gough (minimum  $^{143}\text{Nd}/^{144}\text{Nd}$  is 0.512203), Samoa (0.512287), Pitcairn (0.512333), Heard (0.512483), Hawaii (0.512540), Societies (0.512565), Cape Verde (0.512606), and Comores (0.512630). For two EM hotspots, the three plume catalogs disagree on whether a plume lies beneath the hotspot: San Felix (0.512552) and Meteor-Shona (0.512400). For three other EM hotspots—Rarotonga (0.512629), Amsterdam-

St. Paul (0.512590), and Discovery (0.512207)—Boschi et al. (2007) did not evaluate the presence of plume beneath the hotspot and French and Romanowicz (2015) did not identify a plume. In summary, a majority (~62%) of the hotspots with EM signatures are associated with mantle plumes in all three catalogs, and none of the EM hotspots show an absence of a plume in all three plume catalogs.

While a majority of the EM hotspots are associated with plumes in all three plume catalogs, just nine out of 29 (or ~31%) of the hotspots that exhibit only geochemically depleted  $^{143}\text{Nd}/^{144}\text{Nd}$ —Macdonald (minimum  $^{143}\text{Nd}/^{144}\text{Nd}$  is 0.512687), Marquesas (0.512690), Easter (0.512783), Caroline (0.512924), Azores (0.512667), Canary (0.512740), Cameroon (0.512723), Reunion (0.512772), and Iceland (0.512893)—are associated with plumes in all three plume catalogs. More hotspots exhibiting only geochemically depleted  $^{143}\text{Nd}/^{144}\text{Nd}$  are associated with plumes ( $N = 9$  plumes in all three plume catalogs) than EM hotspots ( $N = 8$  plumes in all three plume catalogs). However, if we account

for the observation that there are over twice as many non-EM hotspots ( $N = 29$ ) as EM hotspots ( $N = 13$ ) in the database of geochemically characterized oceanic hotspots, hotspots that host geochemically enriched  $^{143}\text{Nd}/^{144}\text{Nd}$  (8 plume-related hotspots out of 13 geochemically enriched hotspots, or  $\sim 62\%$ ) are twice as likely to be related to plumes in all three plumes catalogs as hotspots that have only geochemically depleted signatures (9 plume-related hotspots out of 29 geochemically depleted hotspots, or  $\sim 31\%$ ).

While hotspots that sample geochemically enriched domains are more likely to be fed by plumes than hotspots that sample only geochemically depleted mantle domains, it is also true that hotspots associated with mantle plumes are more likely to source enriched mantle signatures than hotspots not associated with plumes. Of the 17 hotspots that overlie mantle plumes in all three plume catalogs, 8 have EM signatures: Societies ( $^{143}\text{Nd}/^{144}\text{Nd} = 0.512565$ ), Hawaii (0.512540), Pitcairn (0.512333), Samoa (0.512287), Cape Verde (0.512606), Comores (0.512630), Heard (0.512483), and Tristan-Gough (0.512203). In contrast, hotspots that are not associated with mantle plumes in any of the three plume catalogs exhibit only non-EM  $^{143}\text{Nd}/^{144}\text{Nd}$  (Fig. 2)—Socorro-Revillagigedo ( $^{143}\text{Nd}/^{144}\text{Nd} = 0.512889$ ), Martin Vas-Trindade (0.512720), Fernando (0.512712), Bowie-Pratt Welker (0.513041), Cobb-Axial-Juan de Fuca (0.513014), and Baja-Guadalupe (0.512887).

Instead of considering all three plume catalogs together (where only hotspots that exhibit agreement on the presence or absence of plumes across all three plume catalogs are taken into account—as we did above), a different approach to evaluating the relationship between plumes and geochemical enrichment at hotspots is to consider each plume catalog individually. We use the method of contingency tables (e.g., Press et al., 1992) to evaluate the probability that the variables—plumes and extreme geochemical enrichment at hotspots—are related. This method is the most suited for this problem because it provides a means to evaluate the association between two variables (i.e., the presence or absence of a plume and whether or not the associated hotspot has geochemically extreme compositions). This method generates a  $p$ -value ranging from 0 to 1. A low  $p$ -value represents a high degree of significance ( $1 - p = \text{significance}$ ) that the presence of a plume is associated with extreme EM signatures at hotspots; high  $p$ -values indicate that any relationship between plumes and geochemical enrichment is more likely to be random. Supplementary Table 3 provides the values used in the contingency table analysis.

Fig. 5 (top panel) shows the number of EM hotspots that are associated with plumes (orange bars) and the number of EM hotspots that are not associated with plumes (blue bars) for each of the three plume catalogs. The fraction above each bar represents the number of EM hotspots divided by the number of plumes (orange bars) or non-plumes (blue bars), and this fraction is expressed as a percentage represented by the height of the bars. For all plume catalogs, a higher fraction of EM hotspots are associated with plumes than with non-plumes. However, the significance of this relationship varies for each plume catalog: For the FR and B-2 catalogs, the significance is only  $\sim 49\%$  and  $57\%$ , respectively, but it is  $95\%$  for the B-1 catalog (percentages are calculated from  $p$ -values in the top panel of Fig. 5, e.g.,  $\sim 49\%$  significance relates to the  $p$ -value of 0.51). Thus, the plumes in the B-1 catalog provide a better prediction of the presence of extreme EM signatures at the associated hotspots than the other two catalogs.

We note that Fig. 5 explores just one of the relationships tested in the contingency table analysis: the fraction of plumes that are EM versus the fraction of non-plumes that are EM. The  $p$ -value resulting from the contingency tables also captures the significance of the observation that a higher fraction of EM hotspots overlie plumes than non-plumes.

#### 4.1.2. $^{206}\text{Pb}/^{204}\text{Pb}$ in mantle-derived hotspot lavas: the distribution of HIMU components in plume-related (and non-plume related) hotspots

With one exception (Discovery hotspot), the maximum  $^{206}\text{Pb}/^{204}\text{Pb}$  values at each of the oceanic hotspots considered here extend above the average  $^{206}\text{Pb}/^{204}\text{Pb}$  value for normal MORB ( $18.30 \pm 0.08$ , 95% confidence; this value excludes back-arc basin basalts and MORB located  $< 500$  km from hotspots; Gale et al., 2013). While all but one of the oceanic hotspots have maximum  $^{206}\text{Pb}/^{204}\text{Pb}$  values that exceed the MORB average, only 13 oceanic hotspots have  $^{206}\text{Pb}/^{204}\text{Pb}$  values  $\geq 20$ .

For 8 of the 13 hotspots that host a lava with  $^{206}\text{Pb}/^{204}\text{Pb} \geq 20$ , all three plume catalogs indicate the presence of a mantle plume (Fig. 2): Macdonald (maximum  $^{206}\text{Pb}/^{204}\text{Pb}$  is 21.65), Azores (20.51), Cameroon (20.52), Easter (20.44), Comores (20.42), Canary (20.27), Cape Verde (20.25), and Marquesas (20.14). However, for three HIMU hotspots, the three plume catalogs disagree on whether a plume lies beneath the hotspot: St. Helena (20.96), Great Meteor-New England (20.44), and Galapagos (20.06). For the Arago hotspot (20.46), Boschi et al. (2007) did not evaluate whether a plume is located beneath the hotspot and French and Romanowicz (2015) did not identify a plume. Finally, in one case—the Baja-Guadalupe hotspot ( $^{206}\text{Pb}/^{204}\text{Pb}$  up to 20.30; e.g., Konter et al., 2009)—a HIMU hotspot is not associated with a plume in any of the plume catalogs. If we consider only the hotspots associated with mantle plumes in all three plume catalogs, which may provide greater confidence regarding the detection of a plume, then the majority of HIMU hotspots—8 of the 13—are sourced by plumes, and only 1 HIMU hotspot is not associated with a plume in any of the plume catalogs.

However, hotspots exhibiting only unradiogenic Pb (non-HIMU) isotopic compositions ( $^{206}\text{Pb}/^{204}\text{Pb} < 20.0$ ) can also be associated with plumes in all three plume catalogs. In fact, more non-HIMU hotspots are associated with plumes ( $N = 9$ ) in all three plume catalogs than HIMU hotspots ( $N = 8$ ), where the plume-related non-HIMU hotspots include Pitcairn (maximum  $^{206}\text{Pb}/^{204}\text{Pb}$  is 19.55), Samoa (19.47), Societies (19.55), Hawaii (18.86), Caroline (18.84), Tristan-Gough (19.86), Iceland (19.31), Reunion (19.17), and Heard (18.83). HIMU hotspots are relatively uncommon (e.g., Stracke, 2012), but it is nonetheless important to account for the observation that there are more than twice as many non-HIMU hotspots ( $N = 29$ ) as HIMU hotspots ( $N = 13$ ) in the database of geochemically characterized oceanic hotspots (Table 2, Fig. 2). When taking into account the unequal distribution of HIMU and non-HIMU hotspots in the oceanic hotspot database, HIMU hotspots are twice as likely (8 out of 13, or 62%, of HIMU hotspots are plume related) as non-HIMU hotspots (9 out of 29, or 31%, of non-HIMU hotspots are plume related) to be associated with plumes in all three plume catalogs.

Hotspots associated with mantle plumes in all three plume catalogs are more likely to exhibit HIMU signatures than hotspots that are not associated with mantle plumes in any of the plume catalogs. Of the 17 hotspots that are associated with mantle plumes in all three catalogs, 8 have HIMU signatures: Macdonald (maximum  $^{206}\text{Pb}/^{204}\text{Pb}$  is 21.65), Easter (20.44), Marquesas (20.14), Azores (20.51), Cameroon (20.52), Comores (20.42), Canary (20.27), Cape Verde (20.25). In contrast, of the six geochemically characterized oceanic hotspots that show agreement on the seismic absence of a mantle plume in all three catalogs—Socorro-Revillagigedo (maximum  $^{206}\text{Pb}/^{204}\text{Pb}$  is 19.15), Martin Vas-Trindade (19.50), Fernando de Noronha (19.57), Bowie-Pratt Welker (19.49), Cobb-Axial-Juan de Fuca (19.54), Baja-Guadalupe (20.30)—only the last-named hotspot has  $^{206}\text{Pb}/^{204}\text{Pb} > 20$  (Fig. 2). Thus, while 8 out of 17 plume-related hotspots have HIMU signatures, only one in six of the non-plume hotspots have HIMU signatures, supporting the hypothesis that plume-related hotspots are more likely

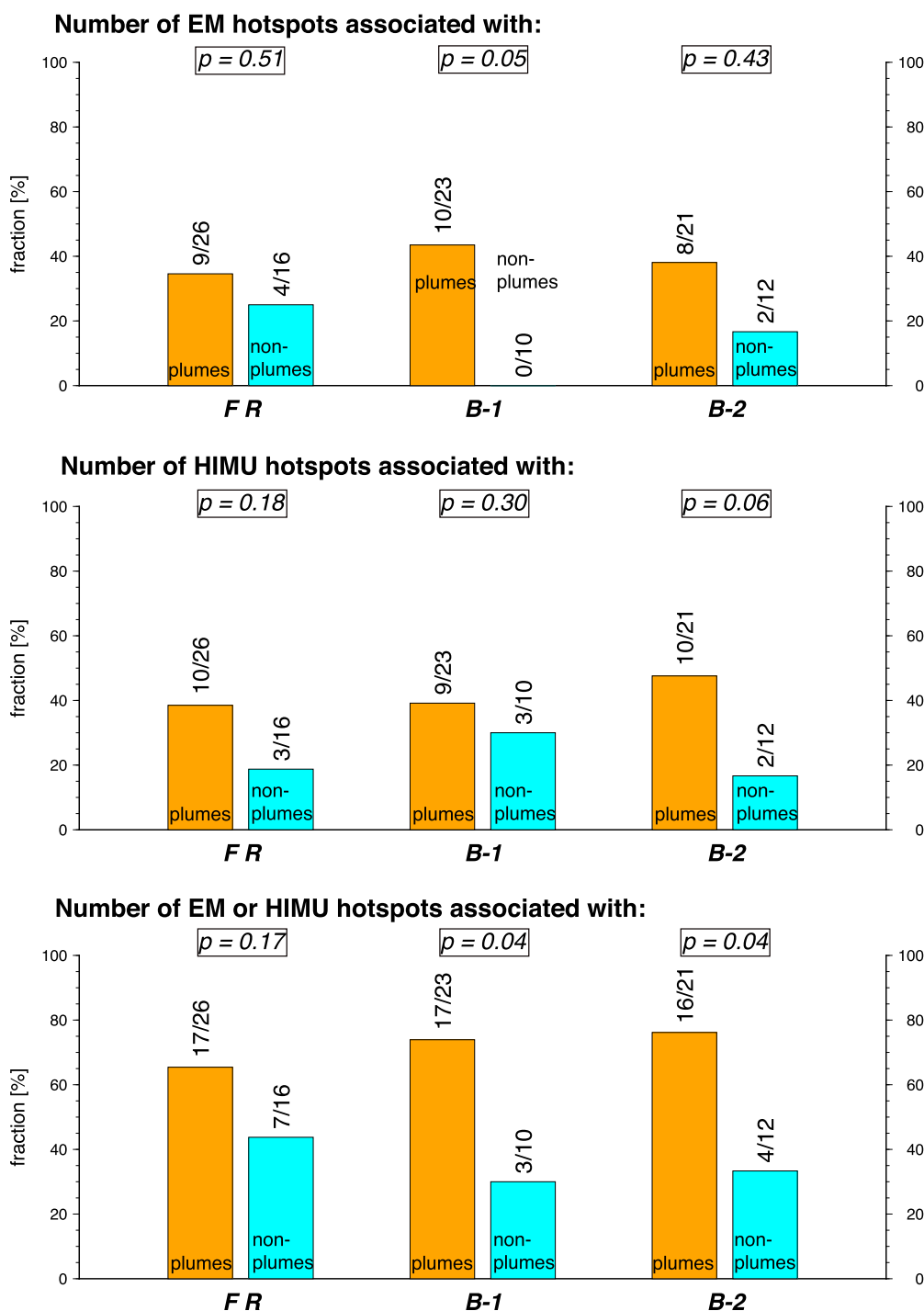


**Fig. 5.** Bar graph plot comparing the number of geochemically extreme hotspots associated with mantle plumes (orange bars) with the number of geochemically extreme hotspots that are not associated with plumes (blue bars). The upper panel explores the lowest  $^{143}\text{Nd}/^{144}\text{Nd}$  compositions at each hotspot (where a hotspot is considered EM if it hosts a lava with  $^{143}\text{Nd}/^{144}\text{Nd} \leq 0.512630$ ), the middle panel explores the highest  $^{206}\text{Pb}/^{204}\text{Pb}$  compositions (where a hotspot is considered HIMU if it hosts a lavas with  $^{206}\text{Pb}/^{204}\text{Pb} \geq 20$ ), and this fraction is expressed as a percentage represented by the height of the bars. The three plume catalogs are examined in turn: the analysis of the French and Romanowicz (FR) catalog is shown in the leftmost orange-blue pair of bars, the Boschi-1 (B-1) catalog in the middle pair of bars, and the Boschi-2 (B-2) catalog in the rightmost pair of bars. The contingency tables method (used to evaluate the probability that the variables, plumes and extreme geochemical enrichment at hotspots, are related) generates  $p$ -values ranging from 0 to 1, and these are shown in the figure (values used in contingency table analyses are provided in Supplementary Table 3). A low  $p$ -value represents a high degree of significance ( $1 - p = \text{significance}$ ) that the presence of a plume is associated with geochemically extreme signatures at hotspots, while high  $p$ -values indicate that any relationship between plumes and geochemical extreme compositions is more likely to be random. For all plume catalogs, a higher fraction of geochemically extreme EM and HIMU hotspots are associated with plumes than with non-plumes, but the significance of this relationship varies depending on the isotopic system (Nd for EM, Pb for HIMU) explored and on the plume catalog used (FR, B-1, B-2). When EM and HIMU signatures are considered together (bottom panel), the significance of the relationship between extreme hotspot geochemistry and mantle plumes is improved (i.e., the lowest  $p$ -values are calculated) for all plume catalogs; note that, in the bottom panel, an inclusive “or” logic is used, so that hotspots with extreme EM only (e.g., Pitcairn), extreme HIMU only (e.g., St. Helena), and extreme EM and HIMU (e.g. Cape Verde) compositions are considered geochemically extreme. (For interpretation of the references to color in this figure, the reader is referred to the web version of this article.)

to sample HIMU compositions than hotspots not associated with plumes.

Contingency tables also show a relationship between extreme HIMU signatures at hotspots and plumes in each plume catalog. Fig. 5 (middle panel) shows that a higher fraction of HIMU hotspots are associated with plumes than with non-plumes in all three plume catalogs, and the significance of this relationship varies for each plume catalog: for the FR and B-1 catalogs, the significance is ~82% and 70%, respectively, but is 94% for the B-2 catalog (see the middle panel of Fig. 5 for *p*-values). Thus, the plumes in the B-2 catalog provide a better prediction for the presence of extreme HIMU signatures at the associated hotspots than the other two catalogs. Another observation is that all three plume catalogs tend to yield a higher overall significance (averaging 82%) for the relationship between plumes and extreme HIMU signatures than the overall significance (averaging 67%) for the relationship between plumes and extreme EM hotspots discussed above.

#### 4.1.3. The combined distribution of EM and HIMU components

We have thus far only considered relationships between plumes and the two extreme hotspot geochemical signatures—EM and HIMU—separately. If EM and HIMU compositions are considered together, we find that the association between plumes and extreme EM and HIMU compositions is even clearer than when EM and HIMU compositions are considered separately. Of the 17 hotspots that are associated with mantle plumes in all three plume catalogs, 14 (or ~82%) have EM or HIMU compositions: six have extreme HIMU compositions (Macdonald, Azores, Easter, Cameroon, Canary, Marquesas), six have extreme EM compositions (Tristan-Gough, Samoa, Pitcairn, Heard, Hawaii, Societies), and two have both extreme EM and extreme HIMU compositions (Cape Verde and Comores). Just three hotspots that are plume-related in all three plume catalogs have neither extreme EM nor extreme HIMU compositions (Reunion, Iceland, Caroline). In contrast, hotspots not associated with plumes in any of the plume catalogs are less likely to host extreme (EM-HIMU) compositions: of the six hotspots that are not associated with plumes in any of the three plume catalogs (Fernando de Noronha, Martin Vaz-Trindade, Cobb-Axial-Juan de Fuca, Bowie-Pratt Welker, Socorro-Revillagigedo, Baja-Guadalupe), only one (Baja-Guadalupe) has an extreme geochemical signature (HIMU), and none of these hotspots have an extreme EM signature.

Hotspots that lack geochemically extreme signatures are also associated with plumes. Three (Iceland, Reunion, and Caroline hotspots) of the 17 (or ~18%) hotspots associated with plumes in all three plume catalogs lack geochemically extreme EM or HIMU compositions. By comparison, hotspots that have extreme geochemical (EM or HIMU) compositions are over three times as likely as hotspots that lack extreme compositions to be associated with plumes in all three plume catalogs: of the 24 hotspots with EM or HIMU compositions, 14 (~58%) are associated with plumes in all three plume catalogs.

Contingency tables also reveal a strong relationship between the presence of plumes and extreme geochemical (EM or HIMU) signatures at hotspots. Fig. 5 (bottom panel) shows that, for each of the plume catalogs, hotspots that have HIMU or EM signatures are much more likely to be associated with plumes than with non-plumes: for the B-1 and B-2 catalogs, the significance of the relationship is 96%, and the significance is 83% for the FR catalog (see the bottom panel of Fig. 5 for *p*-values). Thus, while the data do suggest a relationship between the presence of plumes and extreme EM (section 4.1.1) or HIMU (section 4.1.2) signatures, the significance of the relationship between plumes and extreme geochemical signatures at hotspots increases significantly if hotspots with extreme geochemical signatures—either ex-

treme EM or extreme HIMU signatures, or (in the cases of Cape Verde and Comores) both extreme signatures—are considered together.

## 5. Discussion

### 5.1. Correspondence of extreme EM and HIMU compositions with seismically-constrained plume conduits suggests a deep mantle source for these mantle components

The most extreme EM and HIMU compositions found at the 42 oceanic hotspots examined here tend to sample more extreme EM (lower minimum  $^{143}\text{Nd}/^{144}\text{Nd}$ ) and HIMU (higher maximum  $^{206}\text{Pb}/^{204}\text{Pb}$ ) compositions, respectively, than mean normal MORB compositions. This is consistent with the observation that hotspots sample more geochemically extreme signatures than MORB (e.g., Hart et al., 1973; Zindler and Hart, 1986; Hofmann, 1997). If mid-ocean ridge basalts result from passive melting of the shallow upper mantle, one explanation for the more extreme EM and HIMU compositions at oceanic hotspots is that they sample deeper regions of the mantle than the shallow mantle sampled by mid-ocean ridges.

Consistent with this hypothesis, we find a relationship between geochemically extreme EM or HIMU compositions at hotspots and the presence of seismically-detected mantle plumes beneath the hotspots. A key observation is that hotspots associated with seismically-constrained plumes have a greater likelihood of hosting extreme EM or HIMU signatures than hotspots that are not sourced by plumes (Fig. 5). This observation lends support to the hypothesis that the EM and HIMU domains tend to be deeper than the source for MORB and non-plume hotspots. Otherwise, EM or HIMU compositions would be just as likely to be sampled at hotspots sourced by plumes (which sample the deeper mantle) as by hotspots not sourced by plumes (which sample only the shallow mantle). The strong association between regions of mantle plume upwelling and the presence of geochemically extreme EM or HIMU components in hotspots is not easily explained by models that advocate an upper mantle 'home' for these extreme compositions (Meibom and Anderson, 2003).

In general, hotspots associated with plumes tend to sample either extreme EM or HIMU signatures, but (with the exception of Cape Verde and Comores) not both. Therefore, it is important to consider both EM and HIMU compositions when prospecting for geochemical signatures associated with mantle plumes because these compositions are associated with mantle plumes: when considered together, extreme EM and HIMU signatures at hotspots present a compelling relationship with seismically observed plumes.

The deep mantle sources of plume-fed hotspots are heterogeneous, as shown by the range of radiogenic isotopic compositions—including extreme EM or HIMU components—at most plume-fed hotspots (Supplementary Fig. 1). However, the observation that plume-fed hotspots have either EM or HIMU compositions but (with the exception of two hotspots, Cape Verde and Comores) not both, suggests that the distance between extreme EM and HIMU domains in the deep mantle sources of plumes must generally be too far apart to be sampled by the same plume. Moreover, these domains may arise from subducted crustal sources—including terrigenous silicic sediment, mafic sediment, marine calcareous sediment, and continental and oceanic crust (White and Hofmann, 1982; Hofmann and White, 1982; Castillo, 2015, 2017)—that may become separated in the convecting mantle and, hence, will not always occur in close association in the plume source. Otherwise, we would expect more hotspots to exhibit both EM and HIMU components.

## 5.2. Cases where the relationship between plumes and extreme geochemical (EM or HIMU) compositions break down

While there is a strong association between the presence of mantle plumes and extreme EM or HIMU signatures at hotspots, and an even stronger association between plumes and extreme geochemical signatures when EM and HIMU are considered together, the relationships are not perfect. For example, some plume-related hotspots exhibit no evidence for extreme EM or HIMU geochemical compositions. Similarly, one hotspot with a geochemically extreme signature is not associated with a mantle plume in any of the plume catalogs. Some possible explanations for these observations are discussed below.

### 5.2.1. Why do some plume-related hotspots lack extreme EM or HIMU signatures?

Some plume-related hotspots appear to host only geochemically depleted or non-HIMU signatures. While limited sampling and geochemical characterization of some plume-related hotspots might be an appealing explanation for this observation—whereby additional sampling could hypothetically reveal extreme geochemical compositions—this is unlikely to explain the lack of extreme compositions (EM or HIMU) at two key plume-related hotspots, Iceland and Reunion, which are associated with plumes in all three plume catalogs. Extensive sampling of lavas, covering much of the volcanic history of the Iceland and Reunion hotspots, has failed to reveal extreme EM or HIMU signatures at these plume-related hotspots (note, however, that the third plume-related hotspot lacking EM or HIMU compositions, the Caroline hotspot, has not been extensively sampled for geochemical characterization). Therefore, it is important to understand why some plume-related hotspots do not sample extreme EM or HIMU signatures.

The observation that hotspots overlying seismically detectable plumes do not always host extreme EM or HIMU compositions suggests that, if plumes entrain material from the deep mantle (e.g. Jellinek and Manga, 2004), some regions of the deep mantle sampled by hotspots fed by seismically identified plumes have geochemically extreme EM or HIMU domains, while other regions of the deepest mantle sourcing plumes completely lack geochemically extreme (EM or HIMU) compositions and host only geochemically depleted material.

This hypothesis is supported by prior work, as the deep mantle has long been thought to host depleted domains (e.g., PREMA; Zindler and Hart, 1986) that are juxtaposed with geochemically extreme (EM and HIMU) domains (Li et al., 2014; Garapic et al., 2015). While many plumes are thought to entrain ancient subducted oceanic crust (that evolves into HIMU domains; Hofmann and White, 1982) or ancient subducted continental crust or sediment derived from continental crust (that evolves into EM domains; White and Hofmann, 1982), the bulk of the material in a downgoing plate is composed of depleted mantle lithosphere that will not be the geochemical progenitor of extreme EM or HIMU material (e.g., Castillo, 2015). This depleted oceanic mantle lithosphere material could be preferentially entrained by plumes in lieu of EM and HIMU domains, an effect that may be enhanced if domains composed of depleted mantle lithosphere have lower density than deeply subducted oceanic (e.g., Brandenburg and van Keken, 2007) or continental crust (e.g., Wu et al., 2009) that compose the HIMU and EM domains, respectively.

Additionally, ancient, depleted domains indigenous to the lower mantle, referred to as FOZO (Hart et al., 1992), PHEM (Farley et al., 1992), or C (Hanan and Graham, 1996), are also thought to be entrained by mantle plumes (Mundl et al., 2017), but these depleted domains (which host high  $^3\text{He}/^4\text{He}$ ) may be too dense to be entrained by all but the hottest and most buoyant plumes (Jackson et al., 2017). Plume entrainment of *only* depleted high  $^3\text{He}/^4\text{He}$  man-

tle domains might occur if these depleted domains are occasionally geographically separated from EM and HIMU domains by great distances in the deep mantle. In this case, only depleted domains are entrained and the EM and HIMU reservoirs are too distant from the plume feeding zone to be entrained into the plume. This may help explain why three hotspots associated with seismically-detectable mantle plumes in all three plume catalogs—Iceland, Reunion, and Caroline hotspots—do not convey extreme EM or HIMU material from the deep mantle over the lifetime of these hotspots. However, these three hotspots do entrain an extreme geochemical component characterized by having high  $^3\text{He}/^4\text{He}$ , which supports the hypothesis that elevated  $^3\text{He}/^4\text{He}$  is a geochemical signature associated with mantle plumes.

Thus, while 14 of the 17 hotspots associated with plumes in the three plume catalogs sample either EM or HIMU (or, in the cases of Cape Verde and Comores, both) components, a subset of the 17 plume-related hotspots also sample an extreme mantle component with elevated  $^3\text{He}/^4\text{He}$ . In fact, 13 of the 17 hotspots that are plume-related in all three catalogs host elevated  $^3\text{He}/^4\text{He} \geq 12.6$  Ra, a value that exceeds  $^3\text{He}/^4\text{He}$  typically sampled by MORB ( $8.8 \pm 2.1$  Ra; Graham, 2002): Azores, Cape Verde, Caroline, Easter, Hawaii, Heard, Iceland, Macdonald, Marquesas, Pitcairn, Reunion, Samoa, Societies (see Jackson et al., 2017, for database of maximum  $^3\text{He}/^4\text{He}$  values at hotspots). Therefore, each of the 17 hotspots associated with mantle plumes in all three catalogs sample at least one (and in one case, Cape Verde, all three) of the extreme geochemical components: HIMU, EM, or high  $^3\text{He}/^4\text{He}$ . Together, these three mantle components can be considered to represent “plume signatures”.

### 5.2.2. Geochemically-extreme compositions at hotspots that are not associated with seismically detectable mantle plumes

While most plume-related hotspots have geochemically extreme EM or HIMU compositions, several hotspots with extreme EM or HIMU signatures are not associated with plumes in some of the plume catalogs. In the case of the HIMU Baja-Guadalupe hotspots, a mantle plume is not identified beneath the hotspot in any of the plume catalogs. Critically, this hotspot may no longer be active (Konter et al., 2009). Consequently, the HIMU signature at Baja-Guadalupe may have been sourced from the lower mantle by a plume that is now extinct, and is therefore not detectable with seismic methods.

Alternatively, an upwelling plume is currently located under the Baja-Guadalupe hotspot, but the plume might not have been robustly detected, which may owe to the low buoyancy flux of the plume (which is estimated to be >36 times smaller than that of Hawaii; Konter et al., 2009; King and Adam, 2014). While Boschi et al. (2007) did not consider this hotspot, French and Romanowicz (2015) did suggest the presence of a faint low-velocity conduit offshore of southwestern North America that might be linked to either the Baja-Guadalupe or Yellowstone hotspots. However, French and Romanowicz (2015) indicated that this conduit, if it exists, is beyond the resolution of their study. Thus, it is possible that the extreme HIMU signature at the Baja-Guadalupe hotspot is attributable to a plume.

The case of the Baja-Guadalupe raises an important point about the “non-detection” of a plume: absence of seismic evidence for a plume is not evidence of the absence of a plume. One of French and Romanowicz’s (2015) conclusions is that the plumes they identify are thermochemical plumes, which are wider than thermal plumes (e.g., Kumagai et al., 2008) and are therefore more readily resolvable with seismic methods. In contrast, the conduits of purely thermal plumes may be too narrow to be identified with current seismic tomographic techniques. If this is the case, then purely thermal plumes may be present beneath many hotspots, including the HIMU Baja-Guadalupe hotspot, but these narrow-

conduit thermal plumes remain seismically undetectable. Nonetheless, such purely thermal plumes may be able to entrain geochemically extreme signatures, as is shown by the Baja-Guadalupe hotspot (if, indeed, the hotspot is caused by an upwelling plume).

Some hotspots with EM compositions are not clearly associated with plumes, and this may result from pockets of EM material occasionally residing outside of the lower mantle. Konter and Becker (2012) used a negative correlation between the magnitude of the EM1 component at oceanic hotspots and seismic shear-wave velocity anomalies in the shallow upper to argue that a portion of the EM1 mantle domain may also reside in the shallow mantle. Moreover, the occurrence of EM1 compositions at non-plume “petit spots” (related to tectonically-driven melt extraction processes; e.g. Machida et al., 2015; Hoernle et al., 2011) and isolated seamounts (e.g., Godzilla seamount; Geldmacher et al., 2008) suggests a shallow mantle origin for EM1 at these localities. Although the origin of this extreme signature in the shallow mantle could be the result of the prior passage of an EM1-bearing mantle plume, there is no clear evidence to support this hypothesis. Regardless, the presence of a minor component of EM1 in the shallow mantle could explain the contingency table results (Fig. 5) that show a weaker association between EM hotspots and plumes than the association between HIMU hotspots and plumes.

## 6. Conclusions

Our results contribute to understanding of the geochemical structure of the mantle. The results are consistent with the majority of both extreme HIMU and EM domains compositions being sourced in the deep mantle sampled by plumes. An important caveat is that a minor presence of the EM1 component may reside in the upper mantle. However, the EM1 component is not a common shallow mantle component, as indicated by the observation that this component does not appear in most volcanic systems (non-plume hotspots and MORB) that sample the upper mantle. Instead, EM compositions at hotspots, like HIMU compositions, show a strong association with mantle plumes.

## Acknowledgements

Helpful reviews from Pat Castillo and an anonymous reviewer are acknowledged, as is editorial handling from Tamsin Mather. MGJ acknowledges support from National Science Foundation grants EAR-1624840, OCE-1736984 and EAR-1347377. TWB was partially supported by NSF EAR-1460479. JGK acknowledges partial support from NSF OCE-1538121. MGJ thanks D. Weis, K. Hoernle, J. Geldmacher, J. Barling, C. Beier, L. Vanderkluisen, J. Mata, M. Bizimis, S. Halldórsson and many others who aided in tracking down geochemically extreme lava compositions. The 2016 CIDER program provided resources and inspiration for this interdisciplinary effort.

## Appendix A. Supplementary material

Supplementary material related to this article can be found online at <https://doi.org/10.1016/j.epsl.2017.11.052>.

## References

- Becker, T.W., Boschi, L., 2002. A comparison of tomographic and geodynamic mantle models. *Geochem. Geophys. Geosyst.* 3.
- Bohrson, W.A., Reid, M.R., 1997. Genesis of silicic peralkaline volcanic rocks in an ocean island setting by crustal melting and open-system processes: Socorro Island, Mexico. *J. Pet.* 38, 1137–1166.
- Boschi, L., Becker, T.W., Steinberger, B., 2007. Mantle plumes: dynamic models and seismic images. *Geochem. Geophys. Geosyst.* 7, Q10006.
- Bouvier, A., Vervoort, J.D., Patchett, P.J., 2008. The Lu–Hf and Sm–Nd isotopic composition of CHUR: constraints from unequilibrated chondrites and implications for the bulk composition of terrestrial planets. *Earth Planet. Sci. Lett.* 273, 48–57.
- Brandenburg, J.P., van Keken, P.E., 2007. Deep storage of oceanic crust in a vigorously convecting mantle. *J. Geophys. Res.* 112, B06403.
- Castillo, P., 1988. The Dupal anomaly as a trace of the upwelling lower mantle. *Nature* 336, 667–670. <https://doi.org/10.1038/336667a0>.
- Castillo, P.R., 2015. The recycling of marine carbonates and sources of HIMU and FOZO ocean island basalts. *Lithos* 216, 254–263.
- Castillo, P.R., 2017. An alternative explanation for the Hf–Nd mantle array. *Sci. Bull.* 62, 974–975.
- Farley, K.A., Natland, J.H., Craig, H., 1992. Binary mixing of enriched and undegassed (primitive?) mantle components (He, Sr, Nd, Pb) in Samoan lavas. *Earth Planet. Sci. Lett.* 111, 183–199.
- French, S.W., Romanowicz, B., 2015. Broad plumes rooted at the base of the Earth’s mantle beneath major hotspots. *Nature* 525, 95–99.
- Gale, A., Dalton, C.A., Langmuir, C.H., Su, Y., Schilling, J.-G., 2013. The mean composition of ocean ridge basalts. *Geochem. Geophys. Geosyst.* 14, 489–518. <https://doi.org/10.1029/2012GC004334>.
- Garapic, G., Mallik, A., Dasgupta, R., Jackson, M.G., 2015. Oceanic lavas sampling the high  $^3\text{He}/^4\text{He}$  mantle reservoir: primitive, depleted, or re-enriched? *Am. Mineral.* 100, 2066–2081.
- Geldmacher, J., Hoernle, K., Klügel, A., van den Bogaard, P., Bindeman, I., 2008. Geochemistry of a new enriched mantle type locality in the northern hemisphere: implications for the origin of the EM-I source. *Earth Planet. Sci. Lett.* 265, 167–182.
- Graham, D.W., 2002. Noble gas isotope geochemistry of midocean ridge and ocean island basalts; characterization of mantle source reservoirs. In: Porcelli, D., Balentine, C.J., Wieler, R. (Eds.), *Noble Gases in Geochemistry and Cosmochemistry*. In: *Rev. Mineral. Geochem.*, vol. 47, pp. 247–318.
- Hanan, B.B., Graham, D.W., 1996. Lead and helium isotope evidence from oceanic basalts for a common deep source of mantle plumes. *Science* 272, 991–995.
- Harðardóttir, S., Halldórsson, S.A., Hilton, D.R., 2017. Spatial distribution of helium isotopes in Icelandic geothermal fluids and volcanic materials with implications for location, upwelling and evolution of the Icelandic mantle plume. *Chem. Geol.* 2017. <https://doi.org/10.1016/j.chemgeo.2017.05.012>. In press.
- Hart, S.R., Schilling, J.-G., Powell, J.L., 1973. Basalts from Iceland and along the Reykjanes Ridge: Sr isotope geochemistry. *Nat. Phys. Sci.* 246, 104–107. <https://doi.org/10.1038/physci246104a0>.
- Hart, S.R., 1984. A large-scale isotope anomaly in the Southern Hemisphere mantle. *Nature* 309, 753–757.
- Hart, S.R., 1988. Heterogeneous mantle domains: signatures, genesis and mixing chronologies. *Earth Planet. Sci. Lett.* 90, 273–296.
- Hart, S.R., Hauri, E.H., Oschmann, L.A., Whitehead, J.A., 1992. Mantle plumes and entrainment: isotopic evidence. *Science* 256, 517–520.
- Hoernle, K., Zhang, Y.-S., Graham, D., 1995. Seismic and geochemical evidence for large-scale mantle upwelling beneath the eastern Atlantic and western and central Europe. *Nature* 374, 34–39.
- Hoernle, K., Hauff, F., Werner, R., van den Bogaard, P., Gibbons, A.D., Conrad, S., Müller, R.D., 2011. Origin of Indian Ocean seamount province by shallow recycling of continental lithosphere. *Nat. Geosci.* 4, 883–887.
- Hofmann, A.W., White, W.M., 1982. Mantle plumes from ancient oceanic crust. *Earth Planet. Sci. Lett.* 57, 421–436.
- Hofmann, A.W., 1997. Mantle geochemistry: the message from oceanic volcanism. *Nature* 385, 219–229.
- Jackson, M.G., Konter, J.G., Becker, T.W., 2017. Primordial helium entrained by the hottest mantle plumes. *Nature* 542, 340–343. <https://doi.org/10.1038/nature21023>.
- Jellinek, A.M., Manga, M., 2004. Links between long-lived hot spots, mantle plumes,  $D'$ , and plate tectonics. *Rev. Geophys.* 42, 1–35. RG3002.
- King, S.D., Adam, C., 2014. Hotspot swells revisited. *Phys. Earth Planet. Inter.* 235, 66–83.
- Konter, J.G., Becker, T.W., 2012. Shallow lithospheric contribution to mantle plumes revealed by integrating seismic and geochemical data. *Geochem. Geophys. Geosyst.* 13, Q02004.
- Konter, J.G., Staudigel, H., Blichert-Toft, J., Hanan, B.B., Polve, M., Davies, G.R., Shimizu, N., Schiffman, P., 2009. Geochemical stages at Jasper Seamount and the origin of intraplate volcanoes. *Geochem. Geophys. Geosyst.* 10, Q02001. <https://doi.org/10.1029/2008GC002236>.
- Kumagai, I., Davaille, A., Kurita, K., Stutzmann, E., 2008. Mantle plumes: thin, fat, successful, or failing? Constraints to explain hot spot volcanism through time and space. *Geophys. Res. Lett.* 35. <https://doi.org/10.1029/2008GL035079>.
- Li, M., McNamara, A.K., Garnero, E.J., 2014. Chemical complexity of hotspots caused by cycling oceanic crust through mantle reservoirs. *Nat. Geosci.* 7, 366–370.
- Machida, S., Hirano, N., Sumino, H., Hirata, T., Yoneda, S., Kato, Y., 2015. Petit-spot geology reveals melts in upper-most asthenosphere dragged by lithosphere. *Earth Planet. Sci. Lett.* 426, 267–279.
- Macpherson, C.G., Hilton, D.R., Sinton, J.M., Poreda, R.J., Craig, H., 1998. High  $^3\text{He}/^4\text{He}$  ratios in Manus backarc basin: implications for mantle mixing and the origin of plume in the western Pacific Ocean. *Geology* 26, 1007–1010.

- Meibom, A., Anderson, D.L., 2003. The statistical upper mantle assemblage. *Earth Planet. Sci. Lett.* 217, 123–139.
- Mundl, A., Touboul, M., Jackson, M.G., Day, J.M.D., Kurz, M.D., Lekic, V., Helz, R.T., Walker, R.J., 2017. Tungsten-182 heterogeneity in modern ocean island basalts. *Science* 356, 66–69.
- Press, W.H., Teukolsky, S.A., Vetterling, W.T., Flannery, B.P., 1992. *Numerical Recipes in C: The Art of Scientific Computing*. Cambridge University Press.
- Stracke, A., Hofmann, A.W., Hart, S.R., 2005. FOZO, HIMU, and the rest of the mantle zoo. *Geochem. Geophys. Geosyst.* 6, Q05007. <https://doi.org/10.1029/2004GC000824>.
- Stracke, A., 2012. Earth's heterogeneous mantle: a product of convection-driven interaction between crust and mantle. *Chem. Geol.* 330–331, 274–299.
- White, W.M., 2015. Isotopes, DUPAL, LLSVPs, and Anekantavada. *Chem. Geol.* 419, 10–28.
- White, W.M., Hofmann, A.W., 1982. Sr and Nd isotope geochemistry of oceanic basalts and mantle evolution. *Nature* 296, 821–825.
- Wu, Y., Fei, Y., Jin, Z., Liu, X., 2009. The fate of subducted Upper Continental Crust: an experimental study. *Earth Planet. Sci. Lett.* 282, 275–284.
- Zindler, A., Hart, S., 1986. Chemical geodynamics. *Annu. Rev. Earth Planet. Sci.* 14, 493–571.